ELectronics EXpress

IEICE Electronics Express, Vol.5, No.3, 101–106

Micro-photovoltaic cells designed for magnetotaxis-based controlled bacterial microrobots

Walder André and Sylvain Martel[a)]

NanoRobotics Laboratory, Department of Computer and Software Engineering, and Institute of Biomedical Engineering, École Polytechnique de Montréal (EPM), Campus of the Université de Montréal, Montréal, Canada

a) *sylvain.martel@polymtl.ca*

Abstract: A new architecture allowing an increase of the photocurrent of a photovoltaic cell fabricated with a CMOS 0.18 μm process is described. This cell has been designed specifically to power the onboard electronics of a 400 μm $\times$ 600 μm untethered microrobot propelled by magnetotactic bacteria (MTB). Four cascaded cells of an area of 200 μm $\times$ 200 μm each, provide a short circuit current of 70 μA and an open voltage of 0.48 V from a 555 nm 150 Watts commercial incandescent bulb. Experimental results show a power/area of the photocell of $\sim$110 pW/μm^2.

Keywords: photovoltaic cell, microelectronic, photonic, system-on-chip

Classification: Integrated circuits

References

[1] S. Radovanovic, A. J. Annoma, and B. Nauta, "High-speed, lateral polysilicon photodiode in standard CMOS technology," *Proc. European Solid-State Device Research (ESSDERC'03)*, pp. 521–524, 2003.

[2] Y. Arimata and M. Ehara, "On-chip solar battery structure for CMOS LSI," *IEICE Electron. Express*, vol. 3, no. 13, pp. 287–293, 2006.

[3] A. S. Sedra and K. C. Smith, *Book-Author, Book Title Microelectronic circuits*, 5th ed., Oxford series in electrical and computer engineering, pp. 150–210, 2004.

[4] W. Andre and S. Martel, "Design of photovoltaic cells to power the electronics embedded in an untethered aqueous microrobots propelled by bacteria," *Int. Conf. on Intelligent Robots and Systems (IROS)*, Beijing, China, Oct. 9–15, pp. 1335–1340, 2006.

[5] CMOS 0.18 μm parameters. [Online] http://www.mosis.org

DOI: 10.1587/elex.5.101
Received November 08, 2007
Accepted November 19, 2007
Published February 10, 2008

1 Introduction

CMOS technology has been chosen here to implement low power circuitry to be embedded in a new type of aqueous untethered microrobots. For collecting photons to power the onboard electronics, it is not possible in CMOS technology to build P-I-N photodiodes or resonant cavity photodiodes, but only planar photodiodes. However, planar photodiodes are not as efficient as P-I-N and resonant cavity photodiodes. Typically, the ratio of active area is often responsible for the poor efficiency of the planar photodiodes. They are often made of only one PN-junction and since the diffusion lengths in the P and N-type junctions are small, the output current is decreased accordingly. Few designs in the past have been proposed to improve the active area of the photodiode, such as the lateral polysilicon photodiode with responsivity of 1.20 mA/W [1]. However, because it does not take advantage of the vertically arranged PN-junctions as our proposed architecture does, the responsivity is less than the 5.6 mA/W at 555 nm recorded in our implementation.

Another design is the on-chip solar battery built in CMOS 0.35 μm technology (200 μm $\times$ 500 μm) which does not take into account the lateral PN-junctions that also contribute to the photocurrent, and only produces a short circuit current of $\sim$0.42 μA at 10000 lx optical power [2], whereas our proposed design (200 μm $\times$ 400 μm) provides 1.6 μA at 10000 lx. The proposed architecture makes use of the lateral PN-junctions, which are the P+ and N+ junctions and the vertical PN-junctions, which are the P+ and the N-well junctions and the N+ and the P-substrate junctions as depicted in Fig. 1 (a). The use of CMOS technology to build the battery and power the internal circuit of the microrobot allows the integration over the same substrate of both microelectronic circuits and of the photocell.

2 Proposed architecture for a CMOS planar photocell

The creation of a depletion region occurs when a radiation with sufficient energy falls onto a silicon PN-junction, i.e. when its energy is greater than the energy band gap of the silicon. This is a consequence of the electrons moving from the valence band to the conduction band, therefore generating electron-holes pairs in the depletion region. This region is created without immediate recombination due to the presence of an internal field called built-in voltage potential. The electrons-holes pairs being created will diffuse onto a certain distance called the diffusion lengths L_n and L_p [3]. Therefore, the pairs of electrons-holes which are outside the diffusion zone will not contribute to the external flow of the photonic current since they recombine in the N and P-type semiconductors. Thus, having a very large single PN-junction does not imply that all the area will be used for photonic current conversion. Therefore, here, a new architecture of an on-chip photovoltaic module that allows the creation of more PN-junctions over a given surface area is proposed to increase the generated photocurrent. As depicted in Fig. 1 (a), alternate concentric squares of N and P-type semiconductors are implemented [4]. This particular pattern creates a total of n lateral PN-junctions and $(n+1)$ vertical

DOI: 10.1587/elex.5.101
Received November 08, 2007
Accepted November 19, 2007
Published February 10, 2008

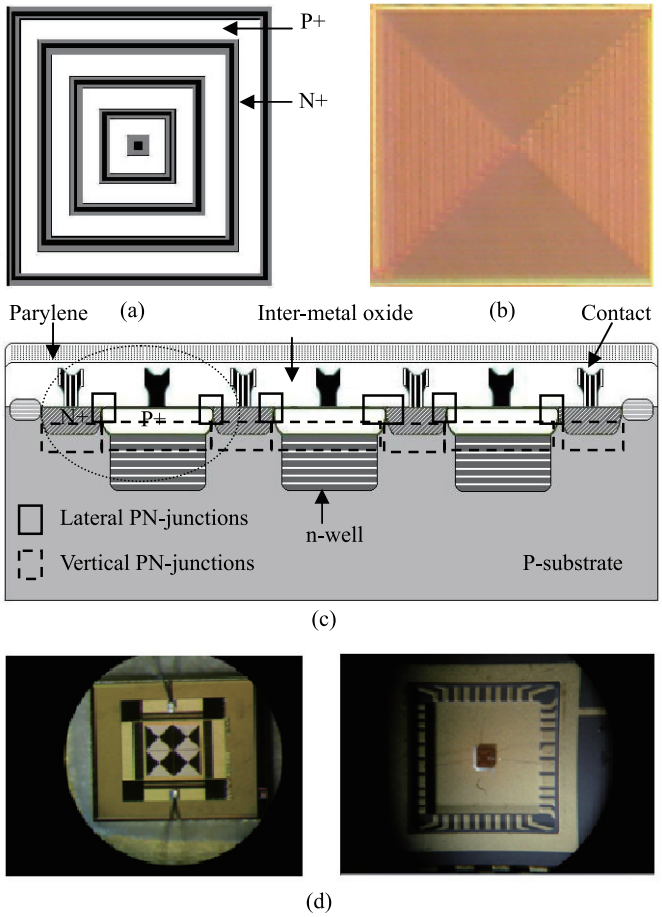

Fig. 1. Proposed architecture: (a) cross-sectional view of the lateral pn-junctions photodiode cell; (b) photomicrograph of the cell (c) cross-sectional view of the cell showing the lateral and the vertical pn-junctions (d) Photomicrograph showing the cell in a package prior testing

PN-junctions. As a result, more depletion areas are obtained, increasing the drift and the diffusion currents. In this architecture, the first square has a surface area of A_0 the second $2A_0$, the third $3A_0$ and so on so that n-th square has a surface area of nA_0. Equation (2) gives the expression for the photonic current, and shows the dependence of the photonic current on the diffusion lengths and the depletion region:

$$I = qG[1A_0 + 2A_0 + 3A_0 + \ldots + (n-1)A_0 + nA_0](L_n + L_p + W_d) \quad (1)$$

$$I = qGA_0\frac{n(n+1)}{2}(L_n + L_p + W_d) \quad (2)$$

where A_0 is the area of the photocell first square from the center and G is the generation rate of holes and electrons pairs estimated to be equal to $3 \times 10^{21}/\mathrm{cm}^3.\mathrm{s}^1$. L_n and L_p are the diffusion lengths in the P and N-type semiconductor, W_d is the depletion width, and n is the number of concentric squares. The total area for one cell is ($200\,\mu\mathrm{m} \times 200\,\mu\mathrm{m}$). Equation (2) takes into account only the lateral PN-junctions. If the vertical PN-junctions are

DOI: 10.1587/elex.5.101
Received November 08, 2007
Accepted November 19, 2007
Published February 10, 2008

considered it becomes:

$$I = qG\left(A_0\frac{n(n+1)}{2} + A_{n0}\sum_0^n 2^i + A_{p0}\sum_0^n 2^i\right)(L_n + L_p + W_d) \qquad (3)$$

where A_{n0} and A_{p0} are the areas of first square from the center of the N+ and P+ layers respectively. Since the doping concentration is the same, the values of L_n, L_p and W_d are the same for both lateral and vertical PN-junctions.

Figure 1 (c) shows the equivalent circuit of the photocell; all the P+ are connected together while all the N+ are connected together via metal one, therefore putting all the created PN-junctions in cascade and increasing the output photonic current. Inside the dash circle are shown the different PN-junctions that can be formed, including lateral and vertical PN-junctions. Figure 1 (d) shows the photovoltaic module that is fabricated. It is able to provide a 70 μA short circuit current and an open voltage of 0.48 V. Figure 2 (a) and 2 (b) show the results obtained for two different sizes of the photovoltaic modules, the first one is 400 μm $\times$ 400 μm and the other one is 200 μm $\times$ 400 μm. However, the voltage provided is not enough to perform a logic function because of the necessary threshold voltages that are

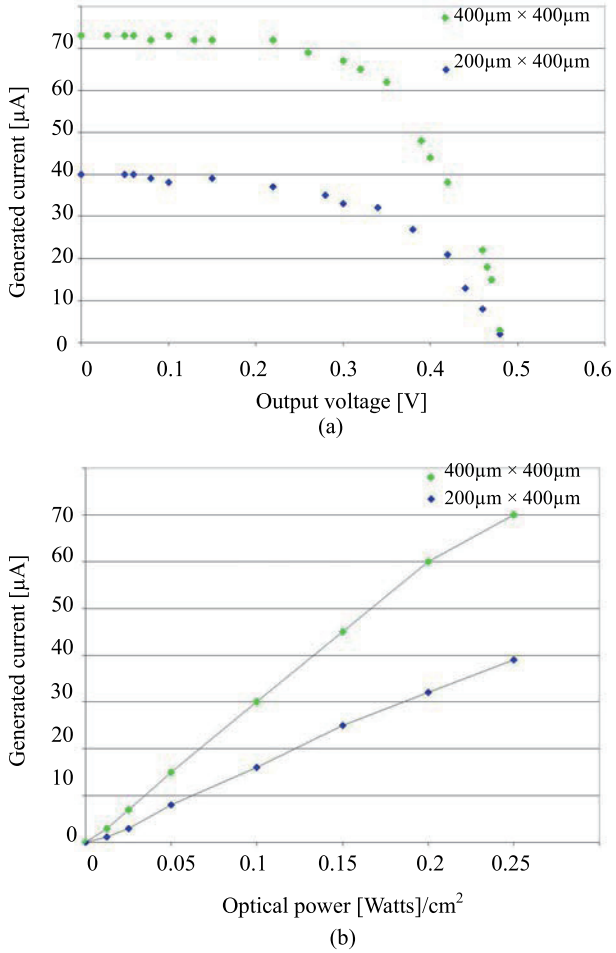

Fig. 2. Experimental results: (a) measured I-V characteristic of the photocell at 0.25 Watt/cm^2 light intensity (b) measured current of the photocell for different light intensities

DOI: 10.1587/elex.5.101
Received November 08, 2007
Accepted November 19, 2007
Published February 10, 2008

approximately equal to 0.5 V and −0.5 V for NMOS and PMOS transistors respectively in CMOS 0.18 μm processes [5]. According to the size constrain, we avoid increasing the size of the photocells which is one way to increase the actual power generated. Accordingly, one approach is to keep the onboard electronics of the microrobot minimal to perform a simple task. Since the microrobot is in die form and intended to operate in an aqueous medium, it is covered with a thin (∼100 nm) transparent layer of parylene. Therefore, we show how light sensitivity has been exploited in order to reduce the threshold voltage of the robot on-chip circuit, and the test results show a decrease in voltage from 0.5 V to 0.25 V.

3 Experimental results

In order to facilitate testing and validation, a DIP package has been used as depicted in Fig. 1 (d). The cell is placed inside an enclosure to avoid ambient light. A 555 nm 150 Watts incandescent lamp is used to illuminate the photocell. A 500 kΩ potentiometer is used to draw the current voltage characteristics of the photocell. A multimeter (Fluke 189) is used to measure the photocurrent while an Agilent 54641 A oscilloscope is used to measure the voltage across the photocell. The measurements are taken within 10 to 15 minutes after the high power of the bulb is switched on in order to avoid overheating the cells.

The measures are taken for two sizes of the proposed photovoltaic modules, which are 400 μm × 400 and 200 μm × 400 μm respectively. Figure 2 (b) shows the measured current of the photocells for different light intensities, while Fig. 3 (a) shows that the 400 μm × 400 μm circuit can operate with a weak incident light, and can produce an output open voltage of ∼400 mV. Figure 3 (b) shows the test result of a VI converter when exposed and then not exposed to an incident light. We see that the circuit begins to operate at a lower threshold voltage (∼0.25 V) than when it was not illuminated (∼0.5 V). This is a result of the accumulation of electrons and holes in the canals of the NMOS and PMOS transistors respectively. This result could be exploited to lower the energy requirement in the implementation of a control system for the microrobot.

4 Conclusion

The experimental results of a new architecture of a photovoltaic circuit fabricated with a CMOS 0.18 μm process are presented. This architecture allows the use of both lateral and vertical PN-junctions. The lateral PN-junctions are formed with the juxtaposition of alternate concentric squares of P and N-types in order to create more PN-junctions over the given surface of the photocell and hence increase the output photonic current. The vertical PN-junctions are formed by the P+ and the N-well, and the N+ with the P-substrate. A short circuit of 70 μA, and an open voltage of 0.48 V are measured for the 400 μm × 400 μm photocell that aims to power the onboard electronics of the untethered microrobot.

DOI: 10.1587/elex.5.101
Received November 08, 2007
Accepted November 19, 2007
Published February 10, 2008

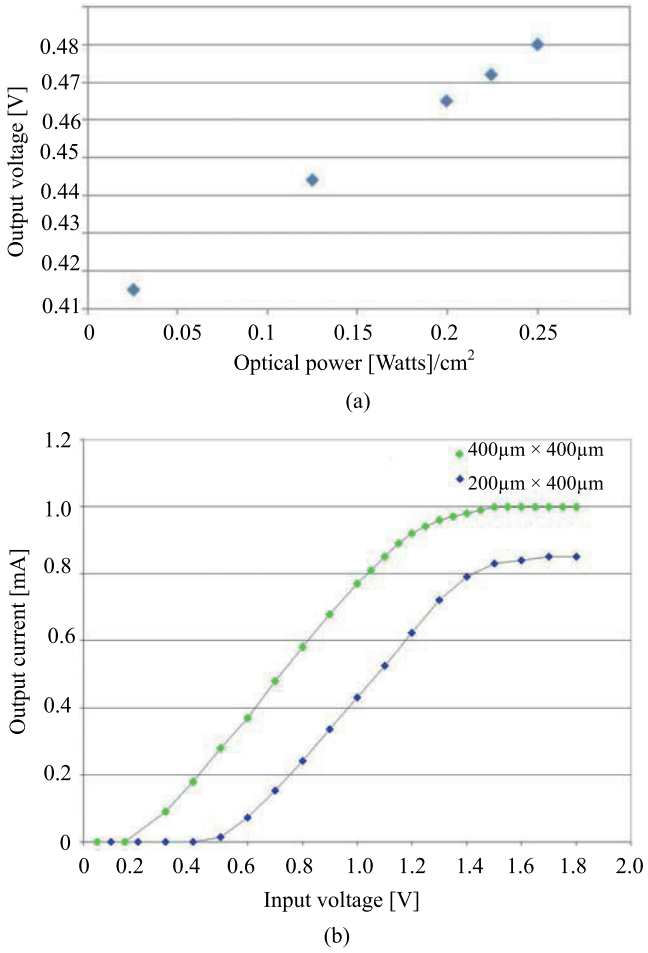

Fig. 3. Experimental results: (a) measured voltage of the photocell for different light intensities (b) measured I-V for the VI converter with and without illuminations

5 Acknowledgements

The project is supported in part by the Canada Research Chair (CRC) in Micro/Nanosystem Development, Fabrication, and Validation, the Canada Foundation for Innovation (CFI), the National Sciences and Engineering Council of Canada (NSERC) and the Government of Québec.

DOI: 10.1587/elex.5.101
Received November 08, 2007
Accepted November 19, 2007
Published February 10, 2008